The low-temperature infrared optical functions of $SrTiO_3$ determined by reflectance spectroscopy and spectroscopic ellipsometry

K. Kamarás,[a] K.-L. Barth, F. Keilmann, R. Henn, M. Reedyk, C. Thomsen, and M. Cardona
Max-Planck-Institut für Festkörperforschung, Heisenbergstrasse 1, D-70569 Stuttgart, Germany

J. Kircher[b] and P. L. Richards
Department of Physics, University of California, and Materials Sciences Division, Lawrence Berkeley Laboratory, Berkeley, California 94720

J.-L. Stehlé
SOPRA, 26 Rue Pierre Joigneaux, F-92270 Bois-Colombes, France

(Received 27 September 1994; accepted for publication 9 March 1995)

By combining reflectance spectroscopy and spectroscopic ellipsometry, the complex dielectric function of $SrTiO_3$ in the frequency range 40–5000 cm^{-1} at 20, 100, 200, and 300 K has been determined. Using a factorized description, analytical expressions for the optical quantities were derived, giving excellent agreement with the experimental data. These can be used for two-layer fits of films on $SrTiO_3$, e.g., of high-T_c superconductors. The fit parameters complement very well those found at higher temperatures. © *1995 American Institute of Physics.*

I. INTRODUCTION

The infrared properties of strontium titanate have been investigated over and over in the last three decades. Early studies contributed essentially to the understanding of soft modes in perovskites.[1] The soft mode has been found in this material to vary in frequency between 4 and 90 cm^{-1}. In addition, there is strong coupling between phonon modes, so that a sum of simple Lorentzian oscillators is unable to describe the phonon spectrum accurately. Several models were proposed to account for coupling[2–4] in order to explain infrared,[6–8] Raman-,[9,10] and neutron-scattering[3,11] results. The most successful mathematical description of the infrared spectra was the factorized form of the dielectric function proposed by Berreman and Unterwald[12] and applied to several perovskite compounds by Gervais and co-workers.[4,5] The latter could successfully fit the infrared reflectance spectra of $SrTiO_3$ from room temperature up to 1200 K.

In the last few years, $SrTiO_3$ has gained additional practical importance as the most widely used substrate for superconducting perovskite films. As experiments on semitransparent samples (insulating phases, films with the c axis in the plane, superlattices, etc.) are becoming more common,[13] it is important to know the substrate dielectric function with very high accuracy in order to model optical processes.[14] However, while detailed studies of other substrates exist,[15,16] no comprehensive experimental investigation on $SrTiO_3$ has been performed in the frequency and temperature range significant for high-T_c research. Sample quality has also improved in recent years, inspired by the high demand, rendering many of the earlier results obsolete.

In this paper, we present the complex dielectric function of $SrTiO_3$ at four temperatures between 20 and 300 K in the entire infrared region (40–5000 cm^{-1}). We performed standard near-normal-incidence reflectance spectroscopy as well as spectroscopic ellipsometry on the same sample, thereby making full use of the advantages and eliminating many of the disadvantages of the two methods. We found that excellent fits to the experimental spectra can be obtained by using the factorized form of the dielectric function. We give a set of parameters at each temperature, which can be used as input for modeling the $SrTiO_3$ substrate in multilayer systems. Our work complements the broad frequency range high-temperature study of Servoin *et al.*,[4] resulting in parameters in general accordance with theirs. The only significant difference is in the linewidth of the soft mode, where our measurement yields a value close to that determined by Raman spectroscopy.

II. EXPERIMENT

The sample was a [100]-oriented, polished circular disk 2.5 cm in diameter and approximately 1 mm thick. This thickness was enough to make the sample opaque throughout the entire measurement range. Reflectance and far infrared ellipsometry measurements were performed by a Bruker 113v Fourier-transform infrared spectrometer. For reflectance spectra (against a gold reference mirror) we used the standard reflectivity insert in combination with a flow-through liquid–He cryostat. Ellipsometry data were obtained by a special rotating analyzer chamber attached to the main instrument with a second cryostat. Details of the setup are described in Ref. 17. The far infrared detector was a silicon bolometer operating at 4 K for both methods; for midinfrared reflectivity, we used a nitrogen-cooled MCT detector. Midinfrared ellipsometry at room temperature was performed by a commercial instrument also operating on the rotating ana-

[a]Permanent address: Research Institute for Solid State Physics, Hungarian Academy of Sciences, P.O. Box 49, Budapest, Hungary H1525.
[b]Present address: Max-Planck-Institut für Festkörperforschung, Heisenbergstrasse 1, D-70569 Stuttgart, Germany. Electronic mail: KIRCHER@CARDIX.MPI-STUTTGART.MPG.DE

 0021-8979/95/78(2)/1235/6/$6.00

lyzer principle, equipped with a custom-made MCT detector.[18] The angle of incidence was 83° in the far infrared and 67° in the midinfrared.

III. DATA ANALYSIS

The purpose of this work is to provide data to be used as input parameters in the analysis of spectroscopic results on multilayer samples including $SrTiO_3$. To this end, we want to maximize both accuracy and signal-to-noise ratio. We tried to do so by using the entire pool of information obtained by reflectance spectroscopy and ellipsometry. Before describing our procedure, we recall some important experimental details.

The standard way to measure reflectivity is to record the intensity of light reflected at near-normal incidence from the sample surface as a function of frequency of the illuminating light, then repeat the same procedure with a reference of well-known and preferably high and featureless reflectivity (metals like aluminum or gold are mostly used for this purpose). The ratio of the two signals, normalized to the known reflectivity of the reference, gives the absolute $R(\omega)$ curve which is then used for Kramers–Kronig (KK) analysis. The first step is to determine the phase shift from the bulk reflectivity,

$$\theta(\omega)=-\frac{\omega}{\pi}P\int_0^\infty \frac{\ln R(\omega')-\ln R(\omega)}{\omega^2-\omega'^2}\,d\omega'. \tag{1}$$

Once the phase shift is known, the dielectric function can be calculated from the following expression:

$$\tilde{\epsilon}=\left|\frac{1+\tilde{r}}{1-\tilde{r}}\right|^2, \quad \tilde{r}=\sqrt{R}e^{i\theta}. \tag{2}$$

Other optical quantities, like the refractive index, absorption coefficient, loss function, etc. follow from $\tilde{\epsilon}$ by straightforward algebraic expressions. In what follows, we will mostly refer to the complex refractive index $\sqrt{\tilde{\epsilon}}=\tilde{n}=n+ik$, frequently used in multilayer modeling.

The error caused in the optical functions by the above calculations depends on the magnitude of R; it has a minimum in the intermediate range $(0.3\leqslant R\leqslant 0.6)$, and increases rather sharply toward lower and higher values. For an ionic crystal such as $SrTiO_3$, which shows strong reststrahlen bands, one encounters both extremes with R spanning the entire range from zero to one.

The exact reproducibility of sample and reference measuring geometry is crucial for the accuracy of the results. This is not an easy task in itself, but becomes even more complicated if one considers the actual circumstances of an infrared experiment. If we want to measure in a wide frequency range [for constructing the integral in Eq. (1) from experimental points wherever possible], several optical components have to be changed along the way (beamsplitters or gratings, sources, filters, detectors, and windows). Most spectra reported in the literature consist in reality of several partial spectra taken in restricted frequency regions with enough overlap to join them smoothly. The merging process involves in the majority of cases a slight rescaling in the overlap region, to avoid sudden jumps which would lead to singularities in the KK results. For carefully controlled alignment and measurement procedures, this scaling does not exceed ±1%, but clearly introduces an arbitrary step in the evaluation, leading to large uncertainties in extreme cases (e.g., when $R\cong 1$). The noise can be kept significantly below this level if the quality of the sample surface, the size of the sample, and the sensitivity of the detector are adequate; random noise can be reduced by increasing the number of scans in an FTIR instrument.

Spectroscopic ellipsometry[19–21] measures the complex reflectivity ratio of incident light polarized parallel (p) and perpendicular (s) to the plane of incidence, under oblique incidence conditions:

$$\tilde{\rho}=\frac{\tilde{r}_s}{\tilde{r}_p}=tg\Psi e^{i\Delta}, \tag{3}$$

where $tg\Psi$ is the amplitude ratio and Δ the relative phase shift. Both instruments used in the present study combine Fourier-transform spectroscopy with rotating analyzer ellipsometry. The sample is illuminated by linearly polarized light (at 45° relative to the plane of incidence) and at several fixed analyzer angles, interferograms are taken and subsequently Fourier-transformed to yield the frequency dependence of the response. Thus Ψ and Δ can be simultaneously determined from the intensity versus analyzer angle data at each frequency. The real and imaginary parts of the dielectric function of the sample are related to Ψ and Δ via straightforward analytical expressions for isotropic samples thicker than the penetration depth[21]—conditions which are fulfilled for our cubic $SrTiO_3$ sample. Ellipsometry requires no reference mirror; thus the accuracy problem mentioned above does not occur; indeed, our Ψ and Δ curves from different beamsplitter regions show perfect overlap. On the other hand, the two polarizers and the large angle of incidence reduce the signal level and consequently the signal-to-noise ratio. Moreover, imperfect (polarization-sensitive) components in the system can lead to false structures in the resulting spectrum.

The procedure we adopted attempts to combine the advantages and eliminate the disadvantages of these two methods, by using the entire set of data obtained on the same sample. Such a set typically consisted of three far infrared parts for both reflectivity and ellipsometry (30–250, 50–400, and 100–650 cm^{-1}), a midinfrared (400–5000 cm^{-1}) part for reflectivity at all temperatures and for ellipsometry at 300 K, and a near infrared part (2000–10 000 cm^{-1}) for reflectivity at 300 K.

First, we calculated the bulk reflectivity from the ellipsometrically determined values of Ψ and Δ. These curves agreed within 0.5% in the overlap regions between the above-mentioned parts. We then scaled each individual part of the reflectance spectrum to match this curve as closely as possible. The broad overlap allowed us further control: if the slopes of the individual curves match, then scaling by a constant is appropriate. We found this to be the case for all our curves, required scaling factors ranging from 1.005 to 1.02. We determined the scaling factors in the areas with the lowest noise of each individual spectral range. This approach

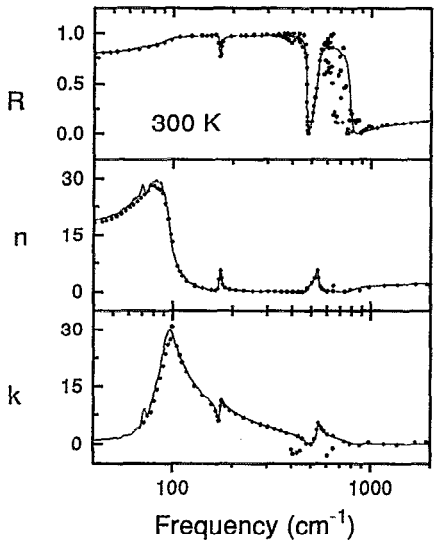

FIG. 1. Bulk normal-incidence reflectivity of $SrTiO_3$ at 300 K calculated from ellipsometry data (points) and measured and scaled to the ellipsometry curve (solid lines). Note the logarithmic frequency scale.

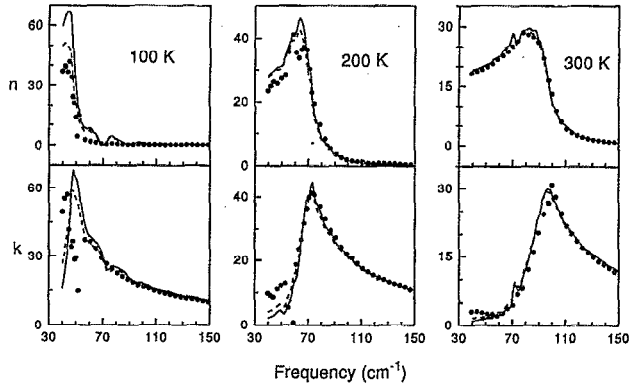

FIG. 2. n and k at 100, 200, and 300 K obtained by ellipsometry (dots) and by KK analysis of reflectivity using two different extrapolations towards zero frequency: R=const. (dashed lines), R determined from Lorentz fit (see Ref. 23) (solid lines).

proved to be fairly reliable, resulting in an overall agreement of the renormalized reflectance curves within 0.5%.

Figure 1 shows the reflectivity curve obtained at 300 K this way, as well as n and k both from Kramers–Kronig analysis of the reflectivity and from direct evaluation of ellipsometry data. The overall agreement is fairly good, and we can clearly identify false structures in both curves. One is the noise peak at 80 cm^{-1} in the reflectivity, amplified in n and k by error propagation. The other one appears in the ellipsometry curve around 400 cm^{-1}, where our instrument had a very low signal level due to an absorption in the detector window. The far and midinfrared ellipsometry data also match well, although the low-frequency region of the latter is very noisy.

In the subsequent fits, we used the renormalized reflectance spectra as input because of the higher signal-to-noise ratio and because they also covered a wide frequency range at low temperatures. Though we took data up to 10 000 cm^{-1} at room temperature and to 5000 cm^{-1} at low temperatures, the reflectivity above 2000 cm^{-1} remained constant. Thus we concentrate in the following on the region 40–2000 cm^{-1}. We want to emphasize that we fitted to R, which is the measured quantity. Consequently, the fit parameters do not depend on details of the Kramers–Kronig transformation. The dependence of the optical functions on these details can be tested by comparing them to the results obtained directly by ellipsometry.

IV. EFFECT OF EXTRAPOLATIONS ON KK ANALYSIS

According to Eq. (1), substantial contributions to $\theta(\omega)$ arise whenever the reflectivity is rapidly changing around ω (the numerator in the integral becomes large) and from frequency regions close to ω (the denominator becomes small). In other words, extrapolations on the low- and high-energy side of the measured range affect mostly the regions which are closest in frequency to the spectral limits. The high-frequency extrapolation is straightforward in our case, because of the constant reflectivity at high frequencies mentioned in the previous paragraph. The contribution of substantially higher lying excitations is merely an additive constant ϵ_∞ to the real part of the dielectric function. We assumed the reflectivity to remain at its 2000–10 000 cm^{-1} level up to 200 000 cm^{-1}, where the free-electron ($R\sim\omega^{-4}$) behavior sets in. On the low-frequency side, one has more choices. Standard low-frequency extrapolations work reasonably well in many well-defined cases. These are the Hagen–Rubens expressions for metals, $R = 1 - A\sqrt{\omega}$, smoothly interpolating to $R=1$ at zero frequency, and the assumption of constant reflectivity for a semiconductor below its gap value or an insulator below its lowest excitation band. If, however, the excitation spectrum is more complicated and/or has features below the lowest measured frequency, then an arbitrary extrapolation can give erroneous results in the optical functions. This point was stressed for high-T_c superconductors by Miller and Richards[22] and Gao *et al.*[23] In our case the problems are caused by the soft mode in $SrTiO_3$, situated right at the low-frequency edge of our measurement range.

Figure 2 shows comparisons of the real and imaginary parts of the complex index of refraction, n and k, respectively, obtained by two different extrapolations, as well as the same quantity determined from Ψ and Δ. In the first case (dashed lines) we took R to be constant at its 40 cm^{-1} value down to zero frequency. In the second case (solid lines), we adopted the extrapolation routine suggested by Gao *et al.*:[23] we performed a simple Lorentzian fit on the optical conductivity determined by an initial KK analysis and used this fit function at low frequency.

At 300 K, the agreement is excellent, independent of the extrapolation, and even at 200 K it is within experimental error. At 100 K, the results are much more sensitive at low frequency, because the soft-mode frequency has decreased. Here we encounter both difficulties mentioned above, namely a rapidly varying reflectance very close in frequency to the onset of the extrapolation. Unfortunately, ellipsometry also has a sensitivity problem here. Since R is close to unity, both Ψ and Δ vary only slowly with variations in the optical

TABLE I. Best fit parameters to Eq. (4) at the four measured temperatures.

	20 K	100 K	200 K	300 K
ω_L	169	170	171	172
γ_L	1.9	2.4	2.6	3.8
ω_T	31	47	69	91
γ_T	1.5	5.7	8.2	15.0
ω_L	475	475	475	474
γ_L	1.9	2.3	2.9	4.5
ω_T	171	172	173	175
γ_T	2.2	1.9	3.3	5.4
ω_L	788	790	790	788
γ_L	18	20	20	25
ω_T	546	546	545	543
γ_T	7.6	8.9	11.0	17.0
ϵ_∞	5.1	5.1	5.1	5.1

functions. This means that small changes in these quantities cause large fluctuations in the results, leading to excessive noise (see the scatter in k in Fig. 2). We encounter this problem under 60 cm^{-1} at 100 K and under 75 cm^{-1} at 20 K. Data below these frequencies are unreliable due to a very poor signal-to-noise ratio. At 20 K the reflectivity stays constant down to our lowest measured frequency and therefore we have no other choice than the first extrapolation.

It is also evident from Fig. 2 that results from different extrapolations are indistinguishable from each other and also from the data determined by ellipsometry above 120 cm^{-1} at all temperatures. It is safe to assume that above this frequency the results of KK transformation represent the true optical functions. Between 40 and 120 cm^{-1} they have to be handled with caution and, of course, points outside the measurement range do not have any physical significance.

V. FITTING PROCEDURE AND RESULTS

Even with the above-mentioned limitations in mind, it is evident that a sum of Lorentzians would give a very poor fit to the n and k curves of Fig. 1. We therefore performed a least-squares fit of the reflectivity between 40 and 2000 cm^{-1} to the following factorized expression which was proven to be successful for strontium titanate at higher temperatures[4] and for the doped material:[5]

$$\tilde{\epsilon}=\epsilon_\infty\prod_j \frac{\omega_{jL}^2-\omega^2+i\gamma_{jL}\omega}{\omega_{jT}^2-\omega^2+i\gamma_{jT}\omega}. \tag{4}$$

We again used the ellipsometry results in choosing some parameters for the fits: from the midinfrared ellipsometry curves, we determine $\epsilon_1(\omega>2000)=5.1$. Since the reflectivity in this spectral region was independent of temperature, we used this as ϵ_∞ without allowing for variation. This agrees with earlier estimates using the refractive index at 5000 cm^{-1}.[24] For the rest of the parameters, we initially took the 300 K values of Servoin *et al.*[4] (the numbers are given in Ref. 5). The fit was very sensitive to the choice of starting values, often giving unphysical results for some of the optical functions.

The parameters yielding the best fits are listed in Table I for all temperatures; we compare measured and fitted reflectivities in Figs. 3 and 4, together with n and k curves. The same comparison is displayed in Figs. 5 and 6 for ϵ_1 and ϵ_2, respectively, in selected frequency regions. We find the

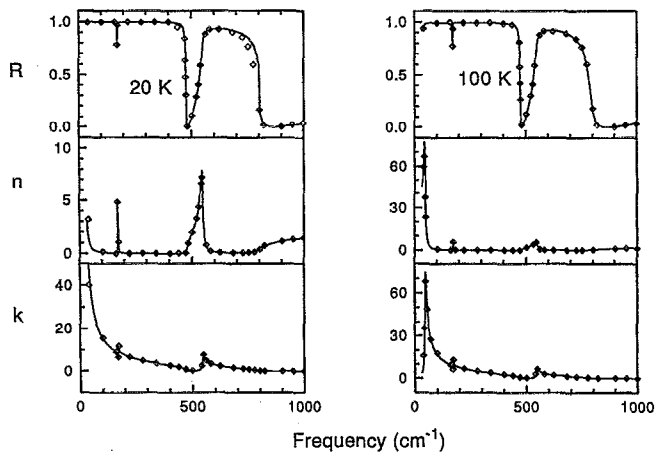

FIG. 3. Reflectivity n and k of $SrTiO_3$ at 20 and 100 K. Symbols are measured reflectivity values and n and k determined from those via KK analysis. Solid lines are calculated by Eq. (4) using the parameters of Table I.

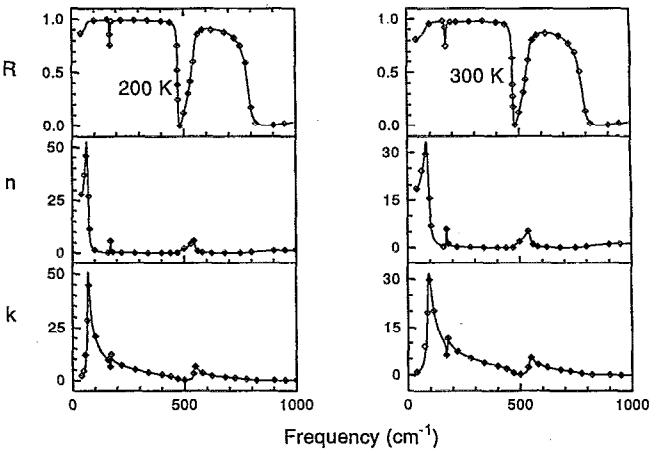

FIG. 4. Same as Fig. 3 at 200 and 300 K.

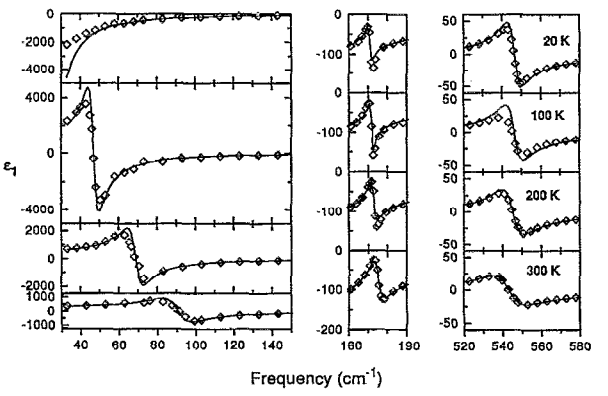

FIG. 5. ϵ_1 of $SrTiO_3$ at 20, 100, 200, and 300 K in selected frequency regions. Symbols as in Fig. 3.

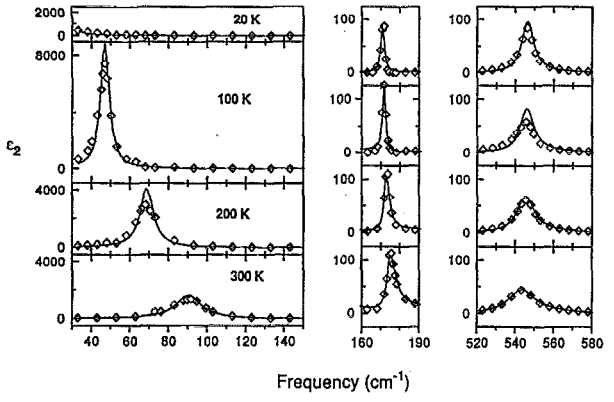

FIG. 6. ϵ_2 of $SrTiO_3$ at 20, 100, 200, and 300 K in selected frequency regions. Symbols as in Fig. 3.

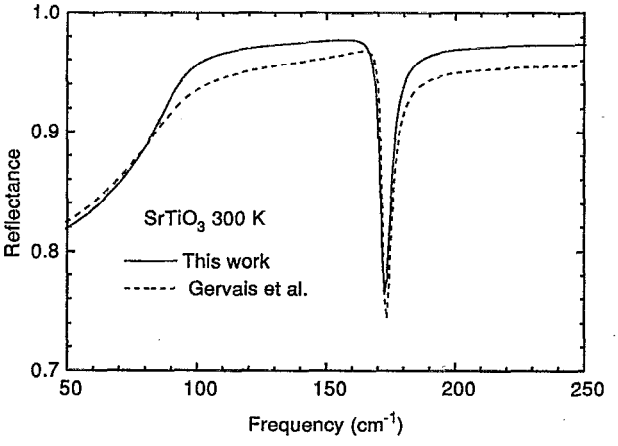

FIG. 7. Reflectivity at 300 K calculated by Eq. (4) using the fit parameters of Ref. 4 (dashed line) and those from this work (solid line).

agreement satisfactory to the extent that we can recommend using analytical expressions based on Eq. (4) to be used for modeling $SrTiO_3$ as substrate in the analysis of multilayers.

It is of interest to compare our results with earlier literature data, especially since there has been a controversy between infrared[7,8] and Raman[9,10] linewidths. Table II summarizes this comparison. Our γ_T values for the soft mode at room temperature are closest to the Raman values determined by Fleury and Worlock[9] and are somewhat lower than those obtained by infrared[4,5,7,8] and hyper-Raman[10] spectroscopy.

Two kinds of explanation have been suggested as to the origin of the discrepancy in linewidths: artifacts in data analysis and unequal sensitivity to surface effects. Fleury and Worlock[9] suggest that the classical three-parameter fits overestimate the damping. We also fitted classical oscillators to our results and while the agreement is indeed poor, they yielded *smaller* instead of larger widths, indicating that at least part of the difference comes from the data themselves. Servoin *et al.*[4] suggest that, since the penetration depth is very small at infrared frequencies due to the strong absorption, deviations from bulk properties caused by imperfections on the surface are more probable. Also, in infrared spectroscopy, the signal is collected from a larger sample area than the laser spot in Raman spectroscopy, so the signal is more likely to contain response from disordered areas. However, hyper-Raman data[10] give an intermediate width for the soft mode; this indicates intrinsic sample differences playing a role besides the methodology.

Though we do not endorse the statement that the large infrared damping constants are the result of improper data manipulation,[1,9] we do believe that the controversy has something to do with the way those parameters are reflected in the measured spectra. We illustrate this point in Fig. 7 by comparing our 300 K reflectance fit with that of Servoin *et al.*[4] The two data sets differ practically only in the value of the soft-mode linewidth. In the Raman spectrum this mode is a distinct peak[9] whose width should be largely independent of extrinsic effects. The signature of the line broadening in the infrared spectra is only a 2% increase in the overall reflectivity level between 100 and 250 cm^{-1}. This value is close to the limits of accuracy one can achieve by reflectance spectroscopy and can reflect slight variations in measurement geometry, sample quality, etc. as discussed above. Our slightly higher R values could be a result of both improved sample quality in comparison with pre-high-T_c materials (we note that they agree with recent high-accuracy reflectivity data[25]), and/or better absolute values using ellipsometry as scaling standard. Although a direct numerical comparison of low-temperature data is not possible (we are not aware of Raman spectra taken at exactly the same temperatures as in the present study), our γ_T values follow precisely the temperature dependence of the Raman parameters, with one exception: the center frequency ω_T at 20 K. Raman spectroscopy yields 14 cm^{-1}; the frequency of 31 cm^{-1} given in Table I yielded the best agreement with the reflectivity, but one has to take into account that our data start only at 40 cm^{-1}. Therefore the fit here is probably not unique. Parameters for the two higher-lying modes complement those found by Servoin *et al.*[4] at high temperature; frequencies and linewidths stay nearly constant and represent the leveling off of the curves shown in Ref. 4.

TABLE II. Phonon parameters determined by various methods for $SrTiO_3$ at 300 K.

	IR Ref. 7	IR Ref. 8	IR Ref. 4	IR this work	Hyper-Raman Ref. 10	Raman Ref. 9
ω_L			172.5	172	175	
γ_L			3	3.8		
ω_T	88	88	89	91	88	90
γ_T	35	44	27	15	23.7	17
ω_L			475	474	266	
ω_L			5	4.5		
ω_T	176	178	175	175	175	
γ_T	7	7	5.5	5.4	6.1	
ω_L			796	788	795	
γ_L			26	25		
ω_T	544	544	544	543	545	
γ_T	32	27	18	17	18	

VI. CONCLUSIONS

We have presented a temperature-dependent study of the dielectric function of $SrTiO_3$ in the infrared. In order to obtain the highest possible accuracy, we used the combination of ellipsometry and reflectance spectroscopy. We derived fit parameters at 20, 100, 200, and 300 K, which can be used in analytical formulas based on the factorized description of the dielectric function to model the optical response of this material when used as a substrate for high-T_c superconductors and other epitaxial films. We obtained values of the soft-mode linewidth closer to the Raman data than earlier reflectivity measurements.

ACKNOWLEDGMENTS

We thank D. Böhme and W. Schlieter for expert technical help. Two of us (J. K. and K. K.) gratefully acknowledge financial support from the Alexander-von-Humboldt Foundation (Bonn, Federal Republic of Germany). This research was also funded by the Bundesminister für Forschung und Technologie (Bonn, Federal Republic of Germany). This work was supported by the Director, Office of Basic Energy Sciences, Materials Sciences Division of the US Department of Energy under Contract No. DE-AC03-76SF00098.

[1] J. F. Scott, Rev. Mod. Phys. **46**, 83 (1974).
[2] R. Migoni, H. Bilz, and D. Bäuerle, Phys. Rev. Lett. **37**, 1155 (1976).
[3] R. A. Cowley, Phys. Rev. **134**, A981 (1964).
[4] J. L. Servoin, Y. Luspin, and F. Gervais, Phys. Rev. B **22**, 5501 (1980).
[5] F. Gervais, J.-L. Servoin, A. Baratoff, J. G. Bednorz, and G. Binnig, Phys. Rev. B **47**, 8187 (1993).
[6] A. S. Barker and M. Tinkham, Phys. Rev. **125**, 1527 (1962).
[7] A. S. Barker, Phys. Rev. **145**, 391 (1966).
[8] W. G. Spitzer, R. C. Miller, D. A. Kleinmann, and L. E. Howarth, Phys. Rev. **126**, 1710 (1962).
[9] P. A. Fleury and J. M. Worlock, Phys. Rev. **174**, 613 (1968).
[10] H. Vogt and G. Rossbroich, Phys. Rev. B **24**, 3086 (1981).
[11] Y. Yamada and G. Shirane, J. Phys. Soc. Jpn. **26**, 396 (1969).
[12] D. W. Berreman and F. C. Unterwald, Phys. Rev. **174**, 791 (1968).
[13] A. M. Rao, P. C. Eklund, G. W. Lehman, D. W. Face, G. L. Doll, G. Dresselhaus, and M. Dresselhaus, Phys. Rev. B **42**, 193 (1990).
[14] P. Calvani, M. Capizzi, S. Lupi, P. Maselli, and E. Agostinelli, Physica C **180**, 116 (1991).
[15] P. Calvani, M. Capizzi, F. Donato, P. Dore, S. Lupi, P. Marselli, and C. P. Varsamis, Physica C **181**, 289 (1991).
[16] S. Cunsolo, P. Dore, S. Lupi, P. Maselli, and C. P. Varsamis, Infrared Phys. **33**, 539 (1992).
[17] K.-L. Barth, D. Böhme, K. Kamarás, F. Keilmann, and M. Cardona, Thin Solid Films **234**, 314 (1993).
[18] J.-L. Stehlé, O. T. Thomas, J. P. Piel, P. Evrard, J. H. Lecat, and L. C. Hammond, Mater. Res. Soc. Symp. Proc. **171**, 349 (1990).
[19] A. Röseler, *Infrared Spectroscopic Ellipsometry* (Akademie, Berlin, 1990).
[20] For most recent developments, see Thin Solid Films **234**, Nos. 1 and 2 (1993).
[21] R. M. A. Azzam and N. M. Bashara, *Ellipsometry and Polarized Light* (North-Holland, Amsterdam, 1977).
[22] D. Miller and P. L. Richards, Phys. Rev. B **47**, 12308 (1993).
[23] F. Gao, D. B. Romero, D. B. Tanner, J. Talvacchio, and M. G. Forrester, Phys. Rev. B **47**, 1036 (1993).
[24] W. L. Bond, J. Appl. Phys. **36**, 1674 (1965).
[25] C. C. Homes, M. Reedyk, D. A. Crandles, and T. Timusk, Appl. Opt. **32**, 2976 (1993).